Predicting Soluble Solids Concentration of 'Geneva 3' Kiwiberries Using Near Infrared Spectroscopy

Aislinn Mumford[1], Zachary Abrahamsson[1], and Iago Hale[1]

Keywords. *Actinidia arguta*, Brix, fruit quality, NIR, postharvest, ripening

Abstract. **Near infrared (NIR) spectroscopy can be applied to nondestructively assess soluble solids concentration (SSC) of ripening, physiologically mature 'Geneva 3' kiwiberries (*Actinidia arguta*). Spectrographic signatures were captured using a handheld NIR produce quality meter to build predictive models of internal fruit quality for 'Geneva 3' kiwiberries that had been held under cold storage (CS) conditions (0 to 1 °C, >90% relative humidity) as well as those not subjected to CS. The CS model, constructed using scans of 133 berries following 4 to 6 weeks in CS, predicts SSC using NIR wavelengths in the range of 729 to 975 nm. A total of 507 berries fresh from the vine were used to construct a predictive model for SSC of non-CS fruit using the same wavelength range. In each case, model predictive performance was investigated using split-half cross-validation, resulting in mean absolute error (MAE) values of 1.2% and 0.8% SSC for the CS and non-CS model, respectively. Each full model was then used to predict SSC of kiwiberries subjected to the alternative CS condition. The non-CS model maintained a low MAE (1.6% SSC) when applied to CS fruit, but the MAE of the CS model applied to non-CS fruit rose considerably (4.5% SSC). The performance of a combined model was tested against both CS and non-CS models, and a benefit to using tailored, CS-specific models was found, particularly in light of cross-seasonal results. As it has proven in many crops, NIR spectroscopy appears to be a promising tool for nondestructively assessing SSC in 'Geneva 3' kiwiberry fruit, with accuracy being enhanced by training models specific to postharvest regimes and/or defined ranges of SSC.**

Although first available for commercial use in the 1980s, near infrared (NIR) technology has only in the past decade been recognized for its potential widespread horticultural applications, ranging from diagnosing crop health to predicting internal fruit quality to facilitating high-speed sorting on packing lines (Walsh et al. 2020a). By illuminating the target fruit with broad-spectrum NIR radiation (780 to 2500 nm) and detecting changes in the spectrum due to interactions with the fruit, NIR spectroscopy makes use of absorbance and/or transmission spectra to provide insights into internal fruit quality (Osborne 2006). An NIR device enables estimation of various quality metrics such as dry matter content and SSC, provided a trained calibration model particular to the cultivar of interest is available (Walsh et al. 2020a). Once such a model has been developed and validated, model coefficients can be shared with others to enable standardized, real-time, nondestructive predictions of essential quality parameters (Kumar et al. 2015).

The ability of NIR technology to gauge internal quality without physically deforming or altogether destroying fruit (McGlone and Kawano 1998) is especially useful in crops that display little or no visual cues to signal physiological maturity or degree of ripeness, whether in the field or on a packing line (Huang 2014). NIR-based technology removes the need for relatively time-intensive destructive sampling, therefore decreasing avoidable losses of good-quality fruit and enabling high-throughput quality-based sorting of marketable produce. Other potential benefits of NIR spectroscopy include low-cost sampling, rapid application, and user convenience, as no sample preparation is required.

Handheld NIR spectrometers have the additional advantage of enabling simple in situ trait monitoring (Kim et al. 2018), a potential convenience to growers who require real-time, high accuracy assessments of fruit quality to guide decision making. For a species like kiwiberry, in which the level of ripeness among berries within a single vine can vary considerably, the ability to perform rapid, nondestructive in situ measurements becomes even more important due to the strong dependence of accuracy on sample size. As temperature can strongly affect the absorbance spectra of fruit, NIR models are often built over a range of temperatures in an effort to calibrate the predictive models for a wide variety of field conditions (Nicolaï et al. 2007). Indeed, many handheld spectrometers come equipped with a built-in thermometer that can measure ambient temperature and adjust model coefficients accordingly.

In addition to in situ applications like monitoring for harvest timing, NIR technology can be integrated into postharvest processes, especially the task of grading and sorting fruit on a packing line. For example, since 2015, NIR spectroscopy has been used to sort kiwifruit (*Actinidia chinensis*) based on predicted dry matter content in New Zealand packing lines (Walsh et al. 2020b). The technology allows millions of individual fruits to be scanned and graded for export, although the automated systems require active management and can have variable accuracy, suggesting room for further improvement (Walsh et al. 2020b). Walsh et al. (2020b) also report that, based on anecdotal evidence, regular bias adjustment and calibration updating may be required to maintain high accuracy of commercial-scale NIR grading systems over multiple weeks, if not days.

Because NIR spectroscopy can provide growers a means of monitoring maturation in the field, the technology

Received for publication 19 Sep 2023. Accepted for publication 19 Jan 2024.

Published online 29 Feb 2024.

[1]Department of Agriculture, Nutrition, and Food Systems, University of New Hampshire, Durham, NH 03824, USA

A.M. and I.H. designed the study, performed data analysis, and contributed to the manuscript. A.M and Z.A. contributed to data collection. We thank the New Hampshire Agricultural Experiment Station for field support.

Partial funding was provided by the New Hampshire Agricultural Experiment Station. This work (scientific contribution number 2991) was supported by the US Department of Agriculture, National Institute of Food and Agriculture Multistate Hatch Project NE9, and the State of New Hampshire.

I.H. is the corresponding author. E-mail: iago.hale@unh.edu.

https://doi.org/10.21273/HORTTECH05316-23

holds promise in the production of kiwiberries (*Actinidia arguta*), small climacteric fruits generally picked when physiologically mature but not yet ripe. Despite its many merits as an emerging specialty crop, kiwiberry does not display any dependable visual "in-field cues" to signal harvesting, meaning time-consuming destructive sampling is typically required to gauge mean SSC and dry matter content, the standard metrics for harvest timing (Mumford et al. 2023). The ability to predict such metrics nondestructively also has the potential to save growers time, enabling more widely representative sampling via a handheld device and preventing losses due to sampling. The development and validation of cultivar-specific models is the necessary first step toward realizing these uses.

The first application of NIR technology in the agricultural field was by Norris (1964), who developed a model to measure the moisture content of bread wheat (*Triticum aestivum*). Following early demonstrations of its usefulness in agronomic crops, horticultural applications of NIR technology increased throughout the 1980s and 1990s, with the development of early models that could predict the dry matter content of onion (*Allium cepa*) (Birth et al. 1985) and moisture content of the cultivated mushroom *Agaricus bisporus* (Roy et al. 1993). NIR technology was first applied to kiwifruit by McGlone and Kawano (1998), who developed a model to nondestructively determine SSC and dry matter content of 'Hayward' kiwifruit using a narrow spectral range of 800 to 1100 nm. Although SSC and dry matter content predictions were satisfactory, fruit firmness predictions were not, despite the presence of firmness-associated pectin in kiwifruit that binds free water and should, in theory, produce a detectable water absorbance band (McGlone and Kawano 1998). Although pectin contributes to the structure and firmness of fruit tissue, it comprises less than 1% of kiwifruit weight, meaning changes in pectin and therefore firmness are difficult to detect with precision (Li et al. 2017). A later model for firmness in 'Hayward' kiwifruit developed by Lee et al. (2012) built on the work of McGlone and Kawano (1998) by including an additional wavelength region of 1108 to 2492 nm, a case study that demonstrates the importance and sensitivity of wavelength selection when constructing models for different quality traits. Because penetration depth of NIR radiation into fruit tissue is wavelength dependent, ensuring use of a range of wavelengths appropriate to the trait can also increase accuracy of predictions (Lammertyn et al. 2000).

Although working NIR models now exist for several cultivars of fuzzy kiwifruit, few models have been developed for cultivars of the much smaller and smooth-skinned kiwiberry. In 2018, Kim et al. attempted to develop a predictive model for dry matter content and SSC in 'Saehan' that had been treated with a Ca-chitosan edible coating. Trained with 100 berries, their model exhibited a prediction coefficient of determination (R^2) value of 0.73. More recently, a similar model was developed by Sarkar et al. (2020) to predict SSC in Autumn Sense, Chungsan, Daesung, and Green Ball cultivars of kiwiberry. Using a partial least squared regression method, the authors obtained R^2 values ranging from 0.37 to 0.59 for the different cultivars.

As the accuracy of NIR spectroscopy models is likely highly cultivar specific (Kim at al. 2018; Peirs et al. 2003), individual models may be required to accurately predict quality traits of select kiwiberry cultivars. Currently, no model exists for Geneva 3 kiwiberry, the recommended cultivar for the northeastern United States (Hastings and Hale 2019; Melo et al. 2017). A working model able to nondestructively predict SSC in 'Geneva 3' kiwiberry could therefore be of benefit to regional growers of this emerging specialty crop. In addition, such an NIR model for 'Geneva 3' could also benefit the larger regional value chain via application in the sorting and grading of fruit for consumers, either within larger operations or in regional packhouses shared by, or contracting from, networks of small-scale producers.

The aims of this study were 2-fold: 1) assess the potential usefulness of NIR technology to predict internal quality metrics of 'Geneva 3' kiwiberry fruits; and 2) determine whether separate models may be required for predicting SSC of fresh fruit vs. fruit that has been subjected to CS conditions. Due to the significant changes in internal composition that CS is known to have on kiwiberries (Sutherland et al. 2017), the initial assumption is that two separate models may be needed, although their cross-application may be possible and should be evaluated. In the end, the non-CS model is envisioned to assist growers in monitoring kiwiberry vines in situ for harvest timing, and the CS model would be useful for nondestructive quality sorting following CS. To the best of our knowledge, the models presented here are the first NIR models developed specifically for 'Geneva 3' kiwiberry, as well as the first to investigate the differential applicability of NIR models to fruit of *Actinidia* sp. before and after CS.

Materials and methods

Plant materials. All fruit used in model training were from cultivar Geneva 3 (USDA PI617133; also CACT80 and DACT229; see Melo et al. 2017) harvested from the Woodman Horticultural Research Farm. The farm, part of the New Hampshire Agricultural Experiment Station, is located on the western side of the campus of University of New Hampshire, Durham, NH, USA (lat. 43°09′06″N, long. 70°56′43″W, elevation 46 m) and has CfB-Charlton fine sandy loam soil. The six vines used in the study were planted in 2013 and have been managed since that time on a T-bar trellis system, as described by Hastings and Hale (2019). The study vines are open pollinated by a large and diverse collection of male (pollenizer) cultivars located throughout the research vineyard, the nearest males being cultivars Meader Male, 74-46, 74-52, and Smith 2 Male.

All fruits used in model building and model validation were harvested from the six vines mentioned previously. The kiwiberries used to train the CS model were harvested between 9 Sep 2020 and 21 Sep 2020, once the fruit of each two-vine block reached the recommended average harvest threshold of 8.0% SSC (Mumford et al. 2023). Because kiwiberry fruits ripen differentially throughout a vine, fruit was harvested randomly throughout the canopies. After harvesting, fruit was washed with tap water to remove surface debris, air dried, and then packed into vented plastic 180-mL clamshells (13 cm × 11 cm × 4 cm). The clamshells were stacked in open bins and held in a cooling tunnel (0 to 1 °C, > 90% relative humidity) within a CS room located on-site at Woodman

Farm for 4 to 6 weeks. The simple cooling tunnel consisted of stainless-steel shelves draped with thick plastic sheets, through which air was continually pulled by a pair of box fans placed at one end to maintain stable air temperature and help disperse any build-up of ethylene gas around the bins of fruit that could accelerate ripening. Ambient temperature was monitored continuously (30-s intervals) via factory-calibrated digital temperature loggers (InTemp model CX403; Onset Computer Corp., Bourne, MA, USA), and relative humidity was monitored weekly via manual sling psychrometer. The fruit exposed to CS conditions that were used to train the postharvest models is hereafter referred to as "CS fruit."

In contrast, the non-CS model was trained exclusively with 'Geneva 3' kiwiberries that had never experienced CS conditions. This fruit, hereafter referred to as "non-CS fruit," was harvested between 3 Sep and 21 Sep of the following season (2021). The fruit was collected for a relatively extended period of the growing season in an effort to capture a wider range of maturities and degrees of ripeness, from physiologically immature to overripe. This range also included the desired SSC for ready-to-eat 'Geneva 3' kiwiberries, which is ~21% SSC (Mumford et al. 2023). In addition to testing predictive accuracy using fruit within the same season and CS conditions, models were also tested on fruit from a third harvest season (2022) that had experienced CS conditions for 5 weeks. These berries were harvested between 24 Sep 2022 and 25 Sep 2022, following the same procedures described previously. Investigating model predictive accuracy on 2022 fruit was intended as a means of evaluating model applicability across growing seasons, especially as kiwiberry has been characterized by considerable seasonal variability in phenolics and nutrient content, which could affect model performance (Latocha et al. 2013).

Spectra acquisition. Spectrographic signatures were captured using a handheld NIR produce quality meter (F-750 Produce Quality Meter; Felix Instruments, Inc., Camas, WA, USA) fitted with its included small fruit adaptor and 19-mm reflector cone. The small fruit adaptor was used to increase the focus of the light source, maximizing the light penetrating the fruit and increasing the penetration depth of the radiation. From both CS and non-CS fruit, all scans were taken after the fruit had stabilized to room temperature (RT) (20 to 25 °C) after a minimum waiting period of 4 h.

To construct the CS model, NIR scans were taken of 133 individual berries at pre-assigned time points (0, 3, 6, and 9 d) as they ripened at RT, between 19 Oct 2020 and 11 Nov 2020. Two scans were taken for each berry, following the practice of using multiple scans to construct models for species with larger fruits like tomato (*Solanum lycopersicum*) (Peiris et al. 1998) and apple (*Malus ×domestica*) (Eisenstecken et al. 2015). However, this practice failed to benefit the resulting CS models, likely because of the fruit's small size, so the scans were manually averaged using a spreadsheet software program (Microsoft Excel 2023; Microsoft Corp., Redmond, WA, USA). The non-CS model was constructed with single scans of 507 kiwiberries picked directly from the vines throughout the season and allowed to stabilize at RT, never experiencing CS. These berries were scanned after temperature stabilization on the day of harvest and not allowed to ripen further at RT.

Table 1 presents summary statistics comparing the kiwiberries used for constructing the two models, along with their respective harvest dates. As shown in Table 1, the fruit used to construct the CS model had a higher overall mean SSC than those used to construct the non-CS model, a result of being picked and subjected to CS only after reaching the minimum mean harvestable threshold of 8.0% SSC, vs. non-CS fruit, which were evaluated across a much broader range of SSC, beginning even before reaching physiological maturity.

Reference measurements. SSC was approximated for each scanned berry by destructively measuring the degrees Brix of its juice with a digital refractometer (PAL-1; Atago Co., Ltd., Tokyo, Japan) immediately following spectra acquisition. Fruits were sliced crosswise with a razor, and the distal half of the fruit, the side farther from the stem, was used to obtain juice.

Spectral data processing and model building. NIR model-building software (Felix Model Building Software, version 1.3.0.192; Felix Instruments, Inc., Camas, WA, USA) was used to construct the models, and spectral preprocessing and model building for both the CS and non-CS models followed the same procedure. Because spectral data preprocessing is required to decrease noise and increase resolution (Sarkar et al. 2020), all absorbance spectra were first converted to their second derivatives. Nonlinear iterative partial least squares regression was then applied to the converted absorbance spectra by the model-building software to identify any potential correlations between the spectra and the reference SSC values. The spectral region used for prediction of SSC in both models was 729 to 975 nm, a "software standard" range that has been shown to accurately predict SSC in many diverse fruits such as apple (Biegert et al. 2021), olive (*Olea europaea*) (Sun et al. 2020), and kiwiberry (Kim et al. 2018). Investigations of alternative ranges, including combinations of noncontiguous windows, supported the vetted 729- to 975-nm range as appropriately informative for SSC. The final models were obtained by weighting each wavelength by its corresponding regression coefficient. By summing the weighted wavelengths and the intercept coefficient, a predicted SSC value can be generated from any spectral scan and compared with the observed SSC value.

Table 1. Summary statistics and harvest dates for the 'Geneva 3' kiwiberries used to construct cold storage (CS)-specific near infrared spectroscopy models for predicting soluble solids content (SSC).

Model	Harvest dates	Sample size (no. of berries)	Wk in CS	SSC range (%)
CS	9 Sep to 21 Sep 2020 (Season 1)	133	4–6	15.0–30.2
Non-CS	3 Sep to 21 Oct 2021 (Season 2)	507	0 (direct from vine)	4.7–27.3

Models were cross-validated using the split-half cross-validation method, also called holdout validation, in which the acquired spectra of half of the samples are randomly chosen to train the model (i.e., training set), which is then used to predict the SSC of the other half (i.e., validation set). In practice, the samples were randomly split into two groups assigning an alternating "1" or "2" to each berry, in simple sequential order. The spectra obtained from the "odd"-numbered berries were used to build the first cross-validation model, which was checked against the "even"-numbered berries, and then vice versa. Finally, to determine whether separate models enhance prediction accuracy of fresh fruit vs. fruit that has been subjected to CS conditions, an additional combined model was constructed by combining the full CS and non-CS model training sets. The performance of this combined model made of the Season 1 CS fruit and the Season 2 non-CS fruit was then compared with the performances of the other two, CS-specific models.

Model construction. Model construction began by importing the acquired spectra into the model-building software, which converts each spectrum to its second derivative. The spectrometer calculates first and second spectral derivatives by applying Savitzky-Golay coefficients, which are widely used to smooth data while retaining signal tendency (Chen et al. 2013; Savitzky and Golay 1964). For model development, a specific wavelength range is selected that performs well in terms of prediction of the trait of interest. Because the wavelength region of 729 to 975 nm has been informatively linked to sugar, carbohydrate, and water absorbance signatures in past studies of various fruits (Scalisi and O'Connell 2021), including kiwiberry (Kim et al. 2018; Sarkar et al. 2020), it is the recommended "standard" range for SSC in the model-building software and was ultimately used in this work. For predicting SSC, the understood benefit of using this relatively narrow range of wavelengths compared with the entire NIR spectrum is that it retains high-influence wavelengths while excluding many low-influence wavelengths, thereby decreasing noise and increasing prediction accuracy. To confirm this, even narrower and wider ranges of wavelengths, including sets of noncontiguous ranges, were also systematically investigated but showed no improvement. In all cases, the resulting models suffered from reduced predictive accuracy and exhibited signs of overfitting, as reflected in the increased number of principal components required to account for observed variation. Noise outside of the chosen wavelength range may be the result of interference from pigments within the visible range (Goke et al. 2018).

Model validation. Principal component analysis (PCA) was conducted to select the optimum number of principal components best able to explain the observed variance in the processed spectra and thereby provide the basis of a predictive model. PCA is a dimensional reduction technique that distills from a large dataset orthogonal combinations of a subset of variables (in this case, specific wavelengths) that best account for the variation among samples without overfitting (i.e., that maximize model fitting while eliminating noise). Model overfitting occurs when a high-dimensional model fits the training set so closely that it fails to accurately predict data outside that set, usually because of the inclusion of higher-order components that account for error variation. In other words, for predictive NIR models, overfitting can happen if too many lower-order (i.e., low signal-to-noise) principal components are included in the model. In this study, the optimal number of principal components used to construct the two models was selected by identifying the point at which an additional principal component decreased the residual root mean square error of cross-validation (RMSECV) by less than 5%.

A properly fitted model generally results in a high R^2 ($R^2 > 0.7$), a high cross-validated coefficient of determination (CVR^2), a low root mean square error (RMSE), and an RMSECV (Felix Instruments 2017). Leave-one-out cross-validation generates the CVR^2 and RMSECV values by systematically removing a spectrum, rebuilding the model without that spectrum, and then using the new model to predict the removed spectrum. This is done for each spectrum in the model and the results are averaged to generate the calibration coefficients. As the R^2 and CVR^2 are influenced by sample size, the metrics of MAE and residual prediction deviation (RPD) were calculated as well. MAE was calculated manually in a spreadsheet and RPD was calculated in the open-source computational programming language R version 4.2.1 (R Core Team 2023) using the RPD function in the package 'chillR' (Luedeling 2023). All figures were generated with the R package 'ggplot2' (Wickham 2016).

Results and discussion

Model construction and validation. Table 2 provides a summary of the NIR calibration values

Table 2. Calibration values for near infrared spectroscopy models developed for predicting soluble solids concentration (SSC) of 'Geneva 3' kiwiberries. The cold storage (CS) models used kiwiberries subjected to CS, the non-CS models used kiwiberries not subjected to CS, and the combined models used both CS and non-CS berries. For both full and split-half cross-validation (SHCV) models, the table presents the numbers of principal components (PCs) retained, the predicted coefficients of determination (R^2), the cross-validated predicted R^2 (CVR^2) values, the root mean square errors of calibration (RMSE), the cross-validated root mean square errors (RMSECV), the mean absolute errors (MAE), and the residual prediction deviations (RPD). The range of wavelengths used for constructing all models was 729 to 975 nm.

Model	PCs	R^2	CVR^2	RMSE [SSC (%)]	RMSECV [SSC (%)]	MAE [SSC (%)]	RPD
CS (full)	4	0.88	0.86	1.35	1.46	0.98	2.95
Non-CS (full)	5	0.95	0.96	1.05	1.08	0.79	4.58
Combined (full)	5	0.96	0.96	1.25	1.29	0.96	5.08
CS (SHCV)	3	0.87	0.84	1.5	1.62	1.20	2.57
Non-CS (SHCV)	5	0.96	0.94	1.1	1.15	0.78	4.72
Combined (SHCV)	5	0.96	0.96	1.26	1.31	1.01	4.79

for the CS, non-CS, and combined models.

Full models. As shown in Table 2, the full non-CS model has higher R^2 and RPD values and lower RMSE and RMSECV values than the full CS model, indications that the non-CS model performs better than the CS model. The lower MAE value further suggests that this improved performance is not simply an artifact of the larger training set of the non-CS model. All models have R^2 values greater than 0.7, a rule-of-thumb minimum R^2 of a model likely to meet performance standards (Felix Instruments 2017). That being said, although R^2 values capture the linear goodness of fit between predicted and measured values, it says nothing about model accuracy, per se. For this, the degree of deviation from perfect prediction, the case where predicted and measured values are equal (not just correlated), is the more informative measure, as captured by a statistic like MAE. Although both models are successful in accounting for variation within their respective training sets (high R^2 values), the non-CS model is more accurate (MAE = 0.79% SSC vs. 0.98% SSC; Fig. 1). The combined model has an MAE of 0.96% SSC, lower than that of the CS model and possibly a result of the disproportionate representation of fruit of lower SSC. Overall, although the full non-CS model exhibits the lowest MAE value, the combined model has the highest RPD value.

Split-half cross-validation models. In practice, the value of such models lies in their ability to predict SSC of berries outside the training sets. To confirm the potential utility of these models to predict SSC in kiwiberries not used in the training sets, split-half cross-validation (SHCV) was conducted (see Materials and methods). As shown in Table 2, when constructed with only half of the spectra and tested with the other half, the R^2 values shifted only slightly from 0.88 to 0.87 and from 0.95 to 0.96 for the CS and non-CS models, respectively. For the combined model, the R^2 value remained steady at 0.96. Similar to the full models, the non-CS SHCV model exhibited the lowest MAE value (0.78% SSC; Fig. 2) and the combined model exhibited the highest RPD value (4.79). In all cases, model building was done as described previously, resulting in the selection of three, five, and five principal components for the CS, non-CS, and combined SHCV models, respectively (Table 2).

Investigating general model applicability. The second objective of this study was to investigate the possibility of a single model (i.e., CS, non-CS, or combined) serving as a suitable universal model for predicting SSC of 'Geneva 3' kiwiberry fruit generally, whether subjected to CS conditions. The applicability of the CS model to kiwiberries that had not experienced CS conditions was tested by comparing the measured SSC of non-CS fruit to the SSC values predicted by the full CS model built using all 133 scans. Although the predicted R^2 of 0.89 indicates that the SSC values predicted by the CS model are highly correlated with the measured SSC of non-CS fruit, the pronounced deviation of the scatter from the line of perfect accuracy, especially for lower SSC values, suggests poor performance (Fig. 3A). This same procedure was followed using the full non-CS model to predict the SSC of CS fruit, resulting in a slightly lower predicted R^2 value of 0.82 but better overall predictive performance (Fig. 3B).

If a model is intended to be used simply to guide vineyard-wide in-field management decisions like timing of harvest, high R^2 values are necessary and may be sufficient. For assessing the quality of individual berries, however, as would be required on a packing line, consideration of an alternative measure of predictive accuracy like MAE (the absolute value of the difference between actual and predicted SSC values) is essential. As shown in Table 3, for non-CS berry SSC

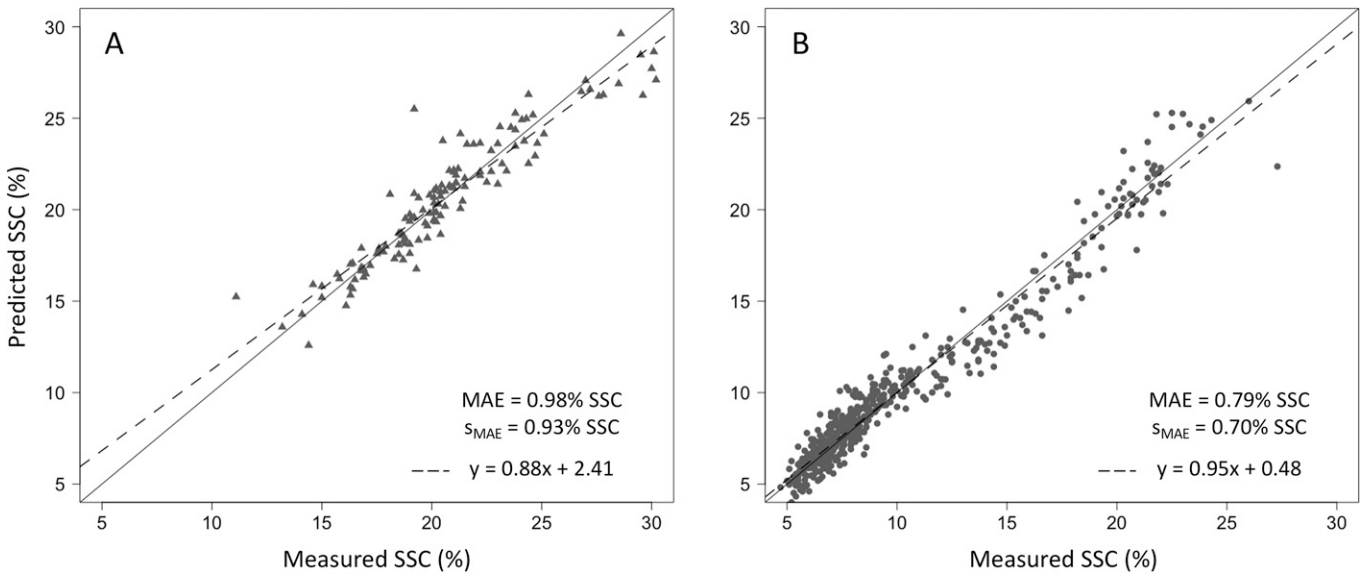

Fig. 1. Scatterplots of predicted vs. measured soluble solid concentration (SSC) of 'Geneva 3' kiwiberries. (A) Results of the full cold storage (CS) model, trained with and applied to a set of 133 berries subjected to CS in Season 1 (2020, triangles). (B) Results of the full non-CS model, trained with and applied to a set of 507 berries never subjected to CS in Season 2 (2021, circles). In each plot, the solid line represents perfect accuracy (predicted = measured), and the dashed line (equation shown) is the linear best fit to the scatter. MAE = mean absolute error. s_{MAE} = standard deviation of the MAE.

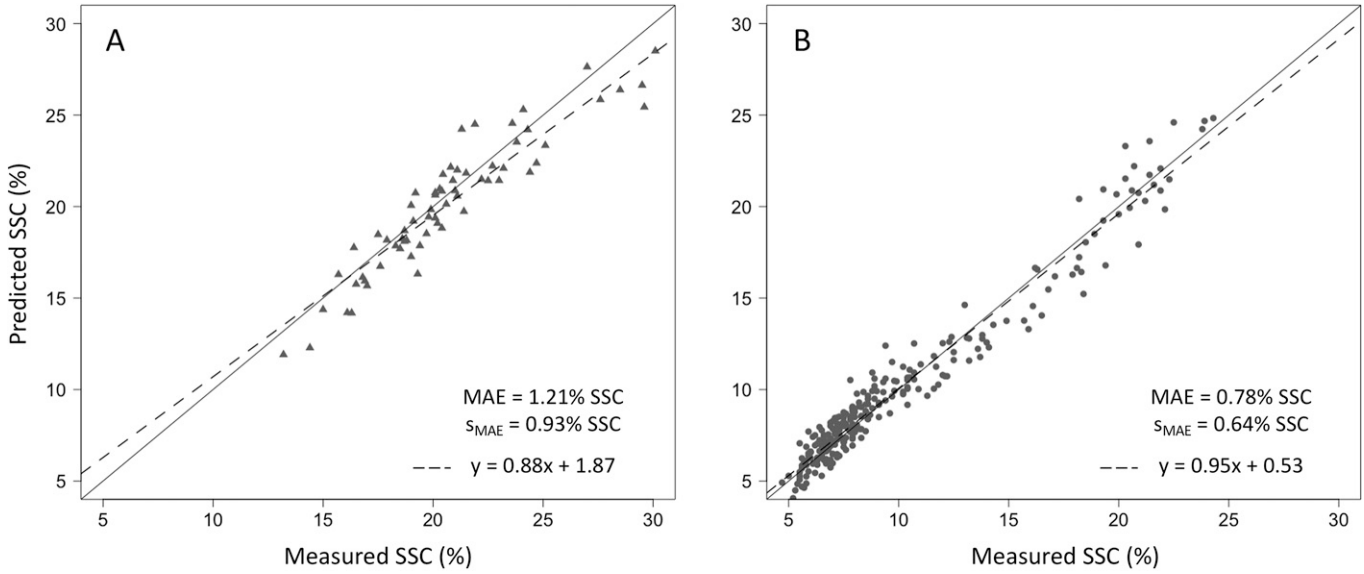

Fig. 2. Scatterplots of predicted vs. measured soluble solid concentration (SSC) of 'Geneva 3' kiwiberries, using the split-half cross-validation (SHCV) method. (A) Results of the SHCV cold storage (CS) model, constructed with 67 randomly chosen berries. (B) Results of the SHCV non-CS model, constructed with 253 randomly chosen berries. In each plot, the solid line represents perfect accuracy (predicted = measured), and the dashed line (equation shown) is the linear best fit to the scatter. MAE = mean absolute error. s_{MAE} = standard deviation of the MAE.

predicted by the full CS model, the mean of this difference (or MAE) was 4.5% SSC with a standard deviation of the MAE (s_{MAE}) of 2.0% SSC, suggesting that the CS model predicts SSC values of individual non-CS fruit relatively poorly. The cross performance of the non-CS model was better, able to predict SSC values of individual CS fruit with an MAE of only 1.6% SSC (s_{MAE} = 1.2% SSC). The combined model, despite its larger training set that included fruit from both CS storage conditions across both seasons, predicted the SSC of berries slightly less accurately than the CS-specific models (see Table 3 and Fig. 4A). Altogether, these results suggest that predictive accuracy may be enhanced through the use of CS-specific models.

Recognizing that the two CS conditions are perfectly confounded with seasonal effects in the above analyses, potentially artificially inflating the importance of CS conditions on model building and unfairly penalizing the

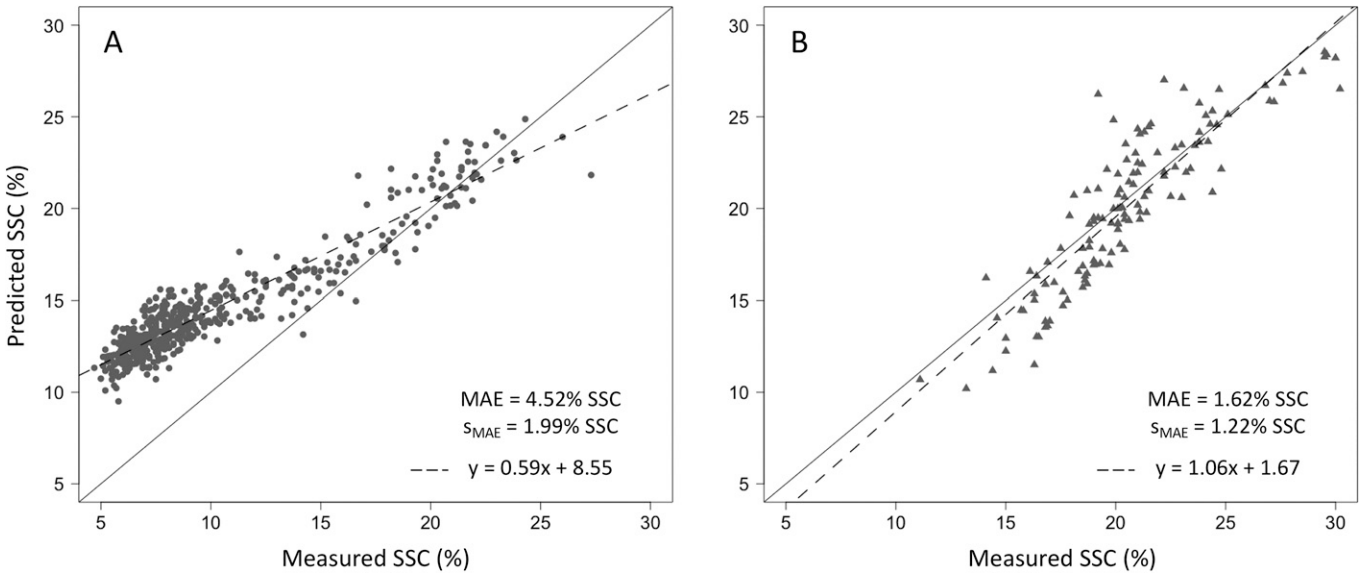

Fig. 3. Scatterplots of predicted vs. measured soluble solids concentration (SSC) of 'Geneva 3' kiwiberries. (A) Results of the full cold storage (CS) model, trained with CS berries from Season 1 (2020) and used to predict the SSC of non-CS fruit from Season 2 (2021, circles). (B) Results of the full non-CS model, trained with non-CS berries from Season 2 (2021) and used to predict the SSC of CS fruit from Season 1 (2020, triangles). In each plot, the solid line represents perfect accuracy (predicted = measured), and the dashed line (equation shown) is the linear best fit to the scatter. MAE = mean absolute error. s_{MAE} = standard deviation of the MAE.

Table 3. Accuracy and precision metrics for predicting the soluble solids concentration (SSC) of individual 'Geneva 3' kiwiberries including mean absolute error (MAE) and its standard deviation (s_{MAE}), for combinations of training and validation sets in this study. The cold storage (CS) models were constructed using kiwiberries harvested during Season 1 (S1, 2020), and the non-CS models were constructed with fruit harvested during Season 2 (S2, 2021). The bottom row presents results from combined models, constructed using both the CS and non-CS training sets. For predictions within season and storage condition, split-half cross-validation (SHCV) results are presented. For all other scenarios, full models are used. Summary statistics of SSC predictions for CS fruit from Season 3 (S3, 2022), not used in any model training, are also included.

	Validation set		
Training set	CS (S1, n = 133)	Non-CS (S2, n = 507)	CS (S3, n = 90)
CS (S1, n = 133)	R^2 = 0.87 MAE = 1.2% SSC s_{MAE} = 0.9% SSC (SHCV)	R^2 = 0.89 MAE = 4.5% SSC s_{MAE} = 2.0% SSC	R^2 = 0.91 MAE = 1.0% SSC s_{MAE} = 0.7% SSC
non-CS (S2, n = 507)	R^2 = 0.82 MAE = 1.6% SSC s_{MAE} = 1.2% SSC	R^2 = 0.96 MAE = 0.8% SSC s_{MAE} = 0.6% SSC (SHCV)	R^2 = 0.90 MAE = 2.2% SSC s_{MAE} = 1.5% SSC
Combined (S1 and S2, n = 640)	R^2 = 0.91 MAE = 1.4% SSC s_{MAE} = 1.0% SSC (SHCV)	R^2 = 0.94 MAE = 0.9% SSC s_{MAE} = 0.8% SSC (SHCV)	R^2 = 0.91 MAE = 1.8% SSC s_{MAE} = 1.1% SSC

universal performance of the combined model, SSC was measured on a small set of available berries in 2022 (Season 3). The 90 berries in this set were randomly harvested from the same 'Geneva 3' vines and held in CS for 5 weeks before measuring SSC, following the same protocols as Season 1.

Although all three models (CS, non-CS, and combined) exhibited high R^2 values ($R^2 \geq 0.9$), the CS model (MAE = 1.0% SSC, s_{MAE} = 0.7% SSC) outperformed both the non-CS model (MAE = 2.2% SSC, s_{MAE} = 1.5% SSC) and the combined model (MAE = 1.8% SSC, s_{MAE} = 1.1% SSC; Fig. 4B) in terms of both accuracy and precision of individual berry prediction. The summarized results in Table 3 indicate that the predictive accuracy and precision of an NIR model for SSC concentration in 'Geneva 3' kiwiberry is higher when applied to fruit subjected to similar CS conditions as the training set, especially when taking seasonal effects into account (always the case, in practice). For this reason, there appears to be a benefit in building separate models for predicting SSC in CS and non-CS fruit. The results in no way negate the possibility of important seasonal effects on model performance, and future work that incorporates scans of fruit from additional seasons and locations is likely to result in even more reliable models. Indeed, despite the inclusion of Season 3 fruit for testing model performance, the constructed models remain confounded within harvest year, underscoring the need for additional data from future harvest seasons to improve generalized performance.

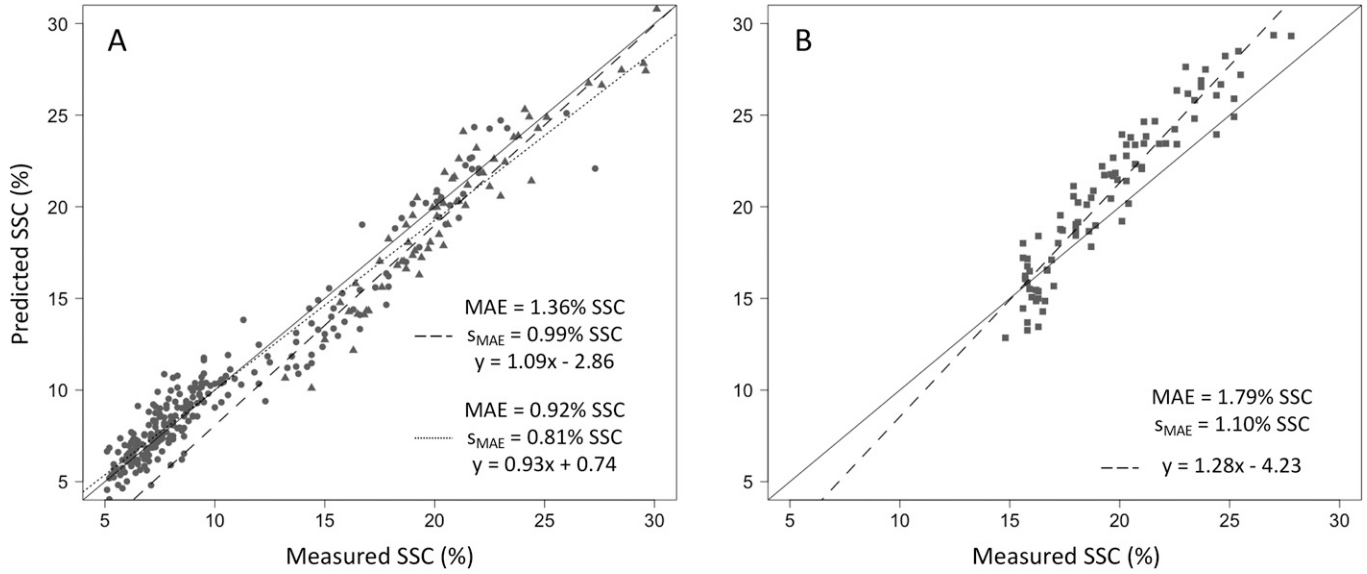

Fig. 4. Scatterplots of predicted vs. measured soluble solids concentration (SSC) of 'Geneva 3' kiwiberries. (A) Results of the split-half cross-validation (SHCV) combined model, constructed with 67 and 253 randomly chosen berries from Seasons 1 (2020 – cold storage; triangles, dashed line) and 2 (2021 – non–cold storage; circles, dotted line), respectively, and used to predict SSC of fruit within the same seasons and storage conditions. (B) Results of the full combined model, constructed with all Season 1 and Season 2 berries and used to predict SSC of Season 3 (2022, squares) fruit that had experienced cold storage. In each plot, the solid line represents perfect accuracy (predicted = measured), and the dotted and dashed lines (equations shown) are the linear best fits to the indicated scatters. MAE = mean absolute error. s_{MAE} = standard deviation of the MAE.

The CS model was designed for quality sorting 'Geneva 3' kiwiberries after CS, and as such, all measurements were taken at a constant temperature. For this initial study, reference measurements for the non-CS model were also taken at RT, so it should be noted that accuracy is likely to be highest when used at or near RT. In other words, neither of these initial models are designed for direct use in the field, under variable temperature conditions. The lack of measurements taken at different temperatures is one limitation of the two models presented here, as temperature fluctuations have been shown to increase NIR model prediction error (Campos et al. 2018). Further development of the models should also incorporate measurements taken under a range of temperatures to reflect the varying temperatures of fruit more accurately in the field.

Conclusions

The results of this study demonstrate the feasibility of building practical models for predicting SSC of 'Geneva 3' kiwiberry fruits and also indicate a possible advantage to developing separate models for fruit that has and has not been subjected to CS conditions. The CS and non-CS models developed here were tested using SHCV, resulting in high R^2 values of 0.87 and 0.96 for the CS and non-CS models, respectively. In terms of predictive accuracy for individual berries within the same season and CS regime (SHCV), consistently low MAE values (1.2% SSC for the CS model; 0.8% SSC for the non-CS model) indicated the potential utility of such models for this important cultivar. The developed model files and regression coefficients, ready for use in compatible NIR devices, are available through the online code and data storage platform GitHub, along with a human-readable (.xlsx) file containing all phenotypic and spectral data for this study, as well as final model coefficients (Hale Laboratory 2023).

Regarding the second objective of the study, which was to ascertain whether different models may improve predictive accuracy of SSC of fruit subjected to different CS conditions, the two models were used to predict the SSC of fruit that had experienced CS conditions contrary to their training sets and the results compared with those from a combined model. The non-CS model was shown to be more widely applicable than the CS model, able to predict the SSC of CS fruit with an MAE of 1.6% SSC, compared with an MAE of 4.5% SSC for non-CS fruit predicted by the CS model. The relative superiority of the non-CS model may be due to its more encompassing training range (4.7% to 27.3% SSC vs. 15.0% to 30.2% SSC), a confounding factor that is discussed in more detail as follows. Despite its much larger training set, though, the non-CS model predicted the SSC of CS fruit from Season 3 with lower accuracy (MAE = 2.2% SSC) than the CS model (MAE = 1.0% SSC). Although seasonal differences likely affect model accuracy to some degree, the preceding results imply that CS treatment may have an even stronger influence. Although the combined model performed rather well in all cases (MAE ranging from 0.9% to 1.8% SSC, across CS conditions), there appears to be a slight but consistent advantage in accuracy when using models tailored to the CS condition of the fruit.

As discussed previously, evaluating the predictive performances of the models on fruit from a different season and outside all training sets (Season 3) is helpful in decoupling the confounded effects of CS and season. CS is confounded with another factor of potential importance, however, namely SSC range. As reflected in Table 1, berries that have been harvested at the recommended SSC threshold (8.0% SSC) and subjected to CS will inevitably exhibit a higher and narrower range of SSC values than berries taken directly from the vine, particularly when monitoring for harvest timing. For this reason, the SSC range of a non-CS training set will largely encompass and therefore represent that of CS fruit; but the converse is not true. This is likely one of the reasons underlying the poor predictive performance of the full CS model on non-CS fruit (Fig. 3A). With a training set consisting of all fruit, the combined model does not suffer from this range restriction. Here, however, a systematic underprediction of midrange SSC values (Fig. 4A) inflates the MAE and suggests that two separate models may indeed still be needed, although it is possible that the distinction between them may be due to SSC range alone (e.g., 5% to 15% SSC vs. 15% to 30% SSC), regardless of postharvest conditions.

The research presented here suggests that NIR spectroscopy may be applied to predict SSC in 'Geneva 3' kiwiberry with a level of precision that is practical for both producers (management decisions) and processors (postharvest sorting and packing), although certainly additional refinement is needed. Future work to improve such predictive models should involve more extensive sampling to capture variation across different seasons, locations (farms), and ambient temperatures. Importantly, this work indicates a slight advantage for separate, CS-specific (or perhaps SSC range-specific) models for 'Geneva 3' kiwiberry and lays the foundation for their improvement based on wider training sets.

References cited

Biegert K, Stöckeler D, McCormick RJ, Braun P. 2021. Modelling soluble solids content accumulation in 'Braeburn' apples. Plants. 10(2):302. https://doi.org/10.3390/plants10020302.

Birth GS, Dull GG, Renfroe WT, Kays SJ. 1985. Nondestructive spectrophotometric determination of dry matter in onions. J Am Soc Hortic Sci. 110:297–303. https://doi.org/10.21273/JASHS.110.2.297.

Campos MI, Antolin G, Debán L, Pardo R. 2018. Assessing the influence of temperature on NIRS prediction models for the determination of sodium content in dry-cured ham slices. Food Chem. 257:237–242. https://doi.org/10.1016/j.foodchem.2018.02.131.

Chen H, Song Q, Tang G, Feng Q, Lin L. 2013. The combined optimization of Savitzky-Golay smoothing and multiplicative scatter correction for FT-NIR PLS models. ISRN Spectrosc. 2013:1–9. https://doi.org/10.1155/2013/642190.

Eisenstecken D, Panarese A, Robatscher P, Huck CW, Zanella A, Oberhuber M. 2015. A near infrared spectroscopy (NIRS) and chemometric approach to improve apple fruit quality management: A case study on the cultivars "Cripps Pink" and "Braeburn". Molecules. 20(8):13603–13619. https://doi.org/10.3390/molecules200813603.

Felix Instruments. 2017. CID bio-science F-750 instruction manual. Camas, WA.

Goke A, Serra S, Musacchi S. 2018. Postharvest dry matter and soluble solids content prediction in d'Anjou and Bartlett pear using near-infrared spectroscopy. HortScience. 53(5):669–680. https://doi.org/10.21273/HORTSCI12843-17.

Hale Laboratory. 2023. NIR-kiwiberry GitHub page. https://github.com/halelab/NIR-kiwiberry/. [accessed 13 Dec 2023].

Hastings W, Hale I. 2019. Growing kiwiberries in New England: A guide for regional producers. http://www.noreastkiwiberries.com. [accessed 4 May 2023].

Huang H. 2014. The genus *Actinidia*: A world monograph. Science Press Beijing, Beijing, China.

Kim JG, Park Y, Shin MH, Muneer S, Lerud R, Michelson C, Kang DI, Min JH, Kumarihami HC. 2018. Application of NIR-spectroscopy to predict the harvesting maturity, fruit ripening and storage ability of Ca-chitosan treated baby kiwifruit. J Stored Prod Postharvest Res. 9(4):44–53. https://doi.org/10.5897/JSPPR2018.0257.

Kumar S, McGlone A, Whitworth C, Volz R. 2015. Postharvest performance of apple phenotypes predicted by near-infrared (NIR) spectral analysis. Postharvest Biol Technol. 100:16–22. https://doi.org/10.1016/j.postharvbio.2014.09.021.

Lammertyn J, Peirs A, De Baerdemaeker J, Nicolaï B. 2000. Light penetration properties of NIR radiation in fruit with respect to non-destructive quality assessment. Postharvest Biol Technol. 18(2):121–132. https://doi.org/10.1016/s0925-5214(99)00071-x.

Latocha P, Wołosiak R, Worobiej E, Krupa T. 2013. Clonal differences in antioxidant activity and bioactive constituents of hardy kiwifruit (*Actinidia arguta*) and its year-to-year variability. J Sci Food Agr. 93(6):1412–1419. https://doi.org/10.1002/jsfa.5909.

Lee J, Kim S, Seong K, Kim C, Um Y, Lee S. 2012. Quality prediction of kiwifruit based on near infrared spectroscopy. Weonye Gwahag Gisulji. 30(6):709–717. https://doi.org/10.7235/hort.2012.12139.

Li M, Pullanagari R, Pranamornkith T, Yule I, East A. 2017. Quantitative prediction of post storage 'Hayward' kiwifruit attributes using at harvest Vis-NIR spectroscopy. J Food Eng. 202:46–55. https://doi.org/10.1016/j.jfoodeng.2017.01.002.

Luedeling E. 2023. chillR: Statistical methods for phenology analysis in temperate fruit trees. R Package Version 0.73.1. http://cran.r-project.org/web/packages/chillR/. [accessed 6 Dec 2023].

McGlone VA, Kawano S. 1998. Firmness, dry-matter and soluble-solids assessment of postharvest kiwifruit by NIR spectroscopy. Postharvest Biol Technol. 13(2):131–141. https://doi.org/10.1016/S0925-5214(98)00007-6.

Melo ATO, Guthrie RS, Hale I. 2017. GBS-based deconvolution of the surviving North American collection of cold-hardy kiwifruit (*Actinidia* spp.) germplasm. PLoS One. 12(1):e0170580. https://doi.org/10.1371/journal.pone.0170580.

Mumford A, Pliakoni ED, Hale I. 2023. Effects of harvest maturity on storability, ripening dynamics, and fruit quality of 'Geneva 3' kiwiberries. HortScience. 58(7):761–767. https://doi.org/10.21273/HORTSCI17105-23.

Nicolaï BM, Beullens K, Bobelyn E, Peirs A, Saeys W, Theron KI, Lammertyn J. 2007. Nondestructive measurement of fruit and vegetable quality by means of NIR spectroscopy: A review. Postharvest Biol Technol. 46(2):99–118. https://doi.org/10.1016/j.postharvbio.2007.06.024.

Norris KH. 1964. Design and development of a new moisture meter. Agric Eng. 45(7):370–372.

Osborne B. 2006. Near-infrared spectroscopy in food analysis. In: Encyclopedia of analytical chemistry. John Wiley & Sons, Hoboken, NJ, USA. https://doi.org/10.1002/9780470027318.a1018.

Peiris KHS, Dull GG, Leffler RG, Kays SJ. 1998. Near-infrared (NIR) spectrometric technique for nondestructive determination of soluble solids content in processing tomatoes. J Am Soc Hortic Sci. 123(6):1089–1093. https://doi.org/10.21273/JASHS.123.6.1089.

Peirs A, Tirry J, Verlinden B, Darius P, Nicolaï BM. 2003. Effect of biological variability on the robustness of NIR models for soluble solids content of apples. Postharvest Biol Technol. 28(2):269–280. https://doi.org/10.1016/S0925-5214(02)00196-5.

R Core Team. 2023. R: A language and environment for statistical computing. R Foundation for Statistical Computing, Vienna, Austria. https://www.R-project.org/. [accessed 6 Dec 2023].

Roy S, Anantheswaran RC, Shenk JS, Westerhaus MO, Beelman RB. 1993. Determination of moisture content of mushrooms by Vis—NIR spectroscopy. J Sci Food Agr. 63(3):355–360. https://doi.org/10.1002/jsfa.2740630314.

Sarkar S, Basak J, Moon E, Kim H. 2020. A comparative study of PLSR and SVM-R with various preprocessing techniques for the quantitative determination of soluble solids content of hardy kiwi fruit by a portable Vis/NIR spectrometer. Foods. 9(8):1078. https://doi.org/10.3390/foods9081078.

Savitzky A, Golay MJE. 1964. Smoothing and differentiation of data by simplified least squares procedures. Anal Chem. 36(8):1627–1639. https://doi.org/10.1021/ac60214a047.

Scalisi A, O'Connell MG. 2021. Application of visible/NIR spectroscopy for the estimation of soluble solids, dry matter and flesh firmness in stone fruits. J Sci Food Agr. 101(5):2100–2107. https://doi.org/10.1002/jsfa.10832.

Sun X, Subedi P, Walker R, Walsh KB. 2020. NIRS prediction of dry matter content of single olive fruit with consideration of variable sorting for normalisation pretreatment. Postharvest Biol Technol. 163:111140. https://doi.org/10.1016/j.postharvbio.2020.111140.

Sutherland PW, Fullerton CG, Schröder R, Hallett IC. 2017. Cell wall changes in *Actinidia arguta* during softening. Scientia Hortic. 226:173–183. https://doi.org/10.1016/j.scienta.2017.08.027.

Walsh KB, Blasco J, Zude-Sasse M, Sun X. 2020a. Visible-NIR 'point' spectroscopy in postharvest fruit and vegetable assessment: The science behind three decades of commercial use. Postharvest Biol Technol. 168:111246. https://doi.org/10.1016/j.postharvbio.2020.111246.

Walsh KB, McGlone VA, Han DH. 2020b. The uses of near infra-red spectroscopy in postharvest decision support: A review. Postharvest Biol Technol. 163:111139. https://doi.org/10.1016/j.postharvbio.2020.111139.

Wickham H. 2016. ggplot2. R Package Version 3.4.4. https://ggplot2.tidyverse.org. [accessed 20 Nov 2023].